THE UNIVERSITY OF MICHIGAN

2778-2-F

RADC-TR-
ASTIA Document No.

STUDIES IN RADAR CROSS SECTIONS XXXVII - ENHANCEMENT OF RADAR CROSS SECTIONS OF WARHEADS AND SATELLITES BY THE PLASMA SHEATH (UNCLASSIFIED REPORT)

by

Charles
C. L. Dolph and H. Weil

December 1959

Report No. 2778-2-F

on

Contract AF 30(602)-1853
Project 5535
Task 45773

Prepared for

ROME AIR DEVELOPMENT CENTER
AIR RESEARCH AND DEVELOPMENT COMMAND
UNITED STATES AIR FORCE
GRIFFISS AIR FORCE BASE, NEW YORK

STUDIES IN RADAR CROSS SECTIONS

I "Scattering by a Prolate Spheroid", F.V. Schultz (UMM-42, March 1950), W-33(038)-ac-14222. UNCLASSIFIED. 65 pgs.

II "The Zeros of the Associated Legendre Functions $P_n^m(\mu')$ of Non-Integral Degree", K.M. Siegel, D.M. Brown, H.E. Hunter, H.A. Alperin and C.W. Quillen (UMM-82, April 1951), W-33(038)-ac-14222. UNCLASSIFIED. 20 pgs.

III "Scattering by a Cone", K.M. Siegel and H.A. Alperin (UMM-87, January 1952), AF-30(602)-9. UNCLASSIFIED. 56 pgs.

IV "Comparison between Theory and Experiment of the Cross Section of a Cone", K.M. Siegel, H.A. Alperin, J.W. Crispin, Jr., H.E. Hunter, R.E. Kleinman, W.C. Orthwein and C.E. Schensted (UMM-92, February 1953), AF-30(602)-9. UNCLASSIFIED. 70 pgs.

V "An Examination of Bistatic Early Warning Radars", K.M. Siegel (UMM-98, August 1952), W-33(038)-ac-14222. SECRET. 25 pgs.

VI "Cross Sections of Corner Reflectors and Other Multiple Scatterers at Microwave Frequencies", R.R. Bonkowski, C.R. Lubitz and C.E. Schensted (UMM-106, October 1953), AF-30(602)-9. SECRET - Unclassified when appendix is removed. 63 pgs.

VII "Summary of Radar Cross Section Studies under Project Wizard", K.M. Siegel, J.W. Crispin, Jr. and R.E. Kleinman (UMM-108, November 1952), W-33(038)-ac-14222. SECRET. 75 pgs.

VIII "Theoretical Cross Section as a Function of Separation Angle between Transmitter and Receiver at Small Wavelengths", K.M. Siegel, H.A. Alperin, R.R. Bonkowski, J.W. Crispin, Jr., A.L. Maffett, C.E. Schensted and I.V. Schensted (UMM-115, October 1953), W-33(038)-ac-14222. UNCLASSIFIED. 84 pgs.

IX "Electromagnetic Scattering by an Oblate Spheroid", L.M. Rauch UMM-116, October 1953), AF-30(602)-9. UNCLASSIFIED. 38 pgs.

X "Scattering of Electromagnetic Waves by Spheres", H. Weil, M.L. Barasch and T.A. Kaplan (2255-20-T, July 1956), AF-30(602)-1070. UNCLASSIFIED. 104 pgs.

XI "The Numerical Determination of the Radar Cross Section of a Prolate Spheroid", K.M. Siegel, B.H. Gere, I. Marx and F.B. Sleator (UMM-126, December 1953), AF-30(602)-9. UNCLASSIFIED. 75 pgs.

XII "Summary of Radar Cross Section Studies under Project MIRO", K.M. Siegel, M.E. Anderson, R.R. Bonkowski and W.C. Orthwein (UMM-127, December 1953), AF-30(602)-9. SECRET. 90 pgs.

XIII "Description of a Dynamic Measurement Program", K.M. Siegel and J.M. Wolf (UMM-128, May 1954), W-33(038)-ac-14222. CONFIDENTIAL. 152 pgs.

XIV "Radar Cross Section of a Ballistic Missile", K.M. Siegel, M.L. Barasch, J.W. Crispin, Jr., W.C. Orthwein, I.V. Schensted and H. Weil (UMM-134, September 1954), W-33(038)-ac-14222. SECRET. 270 pgs.

XV "Radar Cross Sections of B-47 and B-52 Aircraft", C.E. Schensted, J.W. Crispin, Jr. and K.M. Siegel (2260-1-T, August 1954), AF-33(616)-2531. CONFIDENTIAL. 155 pgs.

XVI "Microwave Reflection Characteristics of Buildings", H. Weil, R.R. Bonkowski, T.A. Kaplan and M. Leichter (2255-12-T, May 1955), AF-30(602)-1070. SECRET. 148 pgs.

XVII "Complete Scattering Matrices and Circular Polarization Cross Sections for the B-47 Aircraft at S-band", A.L. Maffett, M.L. Barasch, W.E. Burdick, R.F. Goodrich, W.C. Orthwein, C.E. Schensted and K.M. Siegel (2260-6-T, June 1955), AF-33(616)-2531. CONFIDENTIAL. 157 pgs.

XVIII "Airborne Passive Measures and Countermeasures", K.M. Siegel, M.L. Barasch, J.W. Crispin, Jr., R.F. Goodrich, A.H. Halpin, A.L. Maffett, W.C. Orthwein, C.E. Schensted and C.J. Titus (2260-29-F, January 1956), AF-33(616)-2531. SECRET. 177 pgs.

XIX "Radar Cross Section of a Ballistic Missile II", K.M. Siegel, M.L. Barasch, H. Brysk, J.W. Crispin, Jr., T.B. Curtz and T.A. Kaplan (2428-3-T, January 1956), AF-04(645)-33. SECRET. 189 pgs.

XX "Radar Cross Section of Aircraft and Missiles", K.M. Siegel, W.E. Burdick, J.W. Crispin, Jr. and S. Chapman (WR-31-J, March 1956), SECRET. 151 pgs.

XXI "Radar Cross Section of a Ballistic Missile III", K.M. Siegel, H. Brysk, J.W. Crispin, Jr. and R.E. Kleinman (2428-19-T, October 1956), AF-04(645)-33. SECRET. 125 pgs.

XXII "Elementary Slot Radiators", R.F. Goodrich, A.L. Maffett, N.E. Reitlinger, C.E. Schensted and K.M. Siegel (2472-13-T, November 1956), AF-33(038)-28634, HAC-PO L-265165-F31. UNCLASSIFIED. 100 pgs.

XXIII "A Variational Solution to the Problem of Scalar Scattering by a Prolate Spheroid", F.B. Sleator (2591-1-T, March 1957), AF-19(604)-1949, AFCRC-TN-57-586, AD 133631. UNCLASSIFIED. 67 pgs.

XXIV "Radar Cross Section of a Ballistic Missile - IV The Problem of Defense", M.L. Barasch, H. Brysk, J.W. Crispin, Jr., B.A. Harrison, T.B.A. Senior, K.M. Siegel, H. Weil and V.H. Weston (2778-1-F, April 1959), AF-30(602)-1853. SECRET. 362 pgs.

XXV "Diffraction by an Imperfectly Conducting Wedge", T.B.A. Senior (2591-2-T, October 1957), AF-19(604)-1949, AFCRC-TN-57-591, AD 133746. UNCLASSIFIED. 71 pgs.

XXVI "Fock Theory", R.F. Goodrich (2591-3-T, July 1958), AF-19(604)-1949, AFCRC-TN-58-350, AD 160790. UNCLASSIFIED. 73 pgs.

XXVII "Calculated Far Field Patterns from Slot Arrays on Conical Shapes", R.E. Doll, R.F. Goodrich, R.E. Kleinman, A.L. Maffett, C.E. Schensted and K.M. Siegel (2713-1-F, February 1958), AF-33(038)-28634 and 33(600)-36192; HAC-POs L-265165-F47, 4-500469-FC-47-D and 4-526406-FC-89-3. UNCLASSIFIED. 115 pgs.

XXVIII "The Physics of Radio Communication via the Moon", M.L. Barasch, H. Brysk, B.A. Harrison, T.B.A. Senior, K.M. Siegel and H. Weil (2673-1-F, March 1958), AF-30(602)-1725. UNCLASSIFIED. 86 pgs.

XXIX "The Determination of Spin, Tumbling Rates and Sizes of Satellites and Missiles", M.L. Barasch, W.E. Burdick, J.W. Crispin, Jr., B.A. Harrison, R.E. Kleinman, R.J. Leite, D.M. Raybin, T.B.A. Senior, K.M. Siegel and H. Weil (2758-1-T, April 1959), AF-33(600)-36793. SECRET. 180 pgs.

XXX "The Theory of Scalar Diffraction with Application to the Prolate Spheroid", R.K. Ritt (with Appendix by N.D. Kazarinoff), (2591-4-T, August 1958), AF-19(604)-1949, AFCRC-TN-58-531, AD 160791. UNCLASSIFIED. 66 pgs.

XXXI "Diffraction by an Imperfectly Conducting Half-Plane at Oblique Incidence", T.B.A. Senior (2778-2-T, February 1959), AF-30(602)-1853. UNCLASSIFIED. 35 pgs.

XXXII "On the Theory of the Diffraction of a Plane Wave by a Large Perfectly Conducting Circular Cylinder", P.C. Clemmow (2778-3-T, February 1959), AF-30(602)-1853. UNCLASSIFIED. 29 pgs.

XXXIII "Exact Near-Field and Far-Field Solution for the Back Scattering of a Pulse from a Perfectly Conducting Sphere", V.H. Weston (2778-4-T, April 1959), AF-30(602)-1853. UNCLASSIFIED. 61 pgs.

XXXIV "An Infinite Legendre Integral Transform and Its Inverse", P.C. Clemmow (2778-5-T, March 1959), AF-30(602)-1853. UNCLASSIFIED. 35 pgs.

XXXV "On the Scalar Theory of the Diffraction of a Plane Wave by a Large Sphere", P.C. Clemmow (2778-6-T, April 1959), AF-30(602)-1853. UNCLASSIFIED. 39 pgs.

XXXVI "Diffraction of a Plane Wave by an Almost Circular Cylinder", P.C. Clemmow and V.H. Weston (2871-3-T, September 1959), AF19(604)-4993. AFCRC-TN-59-955. UNCLASSIFIED. 47 pgs.

XXXVII "Enhancement of Radar Cross Sections of Warheads and Satellites by the Plasma Sheath", C.L. Dolph and H. Weil (2778-2-F, December 1959), AF-30(602)-1853. SECRET.

XXXVIII "Non-Linear Modeling of Maxwell's Equations", J.E. Belyea, R.D. Low and K.M. Siegel (2871-4-T, December 1959), AF-19(604)-4993. UNCLASSIFIED.

Preface

This is the thirty-seventh in a series of reports growing out of the study of radar cross sections at The Radiation Laboratory of The University of Michigan. Titles of the reports already published or presently in process of publication are listed on the preceding pages.

When the study was first begun, the primary aim was to show that radar cross sections can be determined theoretically, the results being in good agreement with experiment. It is believed that by and large this aim has been achieved.

In continuing this study, the objective is to determine means for computing the radar cross section of objects in a variety of different environments. This has led to an extension of the investigation to include not only the standard boundary-value problems, but also such topics as the emission and propagation of electromagnetic and acoustic waves, and phenomena connected with ionized media.

Associated with the theoretical work is an experimental program which embraces (a) measurement of antennas and radar scatterers in order to verify data determined theoretically; (b) investigation of antenna behavior and cross section problems not amenable to theoretical solution; (c) problems associated with the design and development of microwave absorbers; and (d) low and high density ionization phenomena.

K. M. Siegel

Table of Contents

On the Change in Radar Cross Section of a Spherical Satellite Caused by a Plasma Sheath +

by

C.L. Dolph, H. Weil

Abstract

A uniform neutral dilute ionized gas is assumed to be perturbed by a sphere moving through it. The radar return from the disturbed region is obtained by integrating the Compton scattering from the electrons, taking phase into account, but ignoring secondary scattering and attenuation. The electron density distribution for this computation is obtained by integration of the zero'th order velocity distribution function for neutral particles obtained by C.S. Wang Chang as a solution of the Boltzmann transport equation.

Numerical results are obtained for the perturbation of the electron distribution by a sphere traveling at 8 km/sec and an altitude of 500 km, and for the radar cross section of this perturbed region when viewed broadside. ++

+ This portion of the final report consists essentially of a paper presented at the Symposium on the Plasma Sheath; Its Effects on Communication and Detection, sponsored by AFCRC in December 1959. The changes are in Part III which has been expanded here to include more extensive numerical results on radar cross sections.

++ The theoretical work and preliminary computations were supported by USAF Contract AF 30(602)-1853. The final machine computations were carried out as an unsponsored faculty research project MO2-N at the Computation Laboratory of The University of Michigan.

Introduction

A sphere is assumed to move with a constant velocity, V, through a dilute, electrically neutral, ionized gas which, in its unperturbed state, is assumed to have a uniform number distribution of electrons, n. The sphere disturbs the distribution of electrons to a non-uniform one, N, with an excess ahead of the sphere and a deficiency behind it. The simplest estimate of the effect of this non-uniform, but everywhere dilute distribution on the radar return is obtained by summing the scattering by the individual electrons accelerated by the incident field. Electrons only are considered since their return is far greater than that of the much heavier positive ions, or the Rayleigh scattering from non-ionized particles. The incident field on each electron is assumed to be a plane wave; this implies that secondary scattering is ignored. The approach is thus directly analogous to that used to determine the radar return from underdense meteor trails [1].

There are three parts to the paper. The first part consists of a formulation of the expression for the backscattered energy. This expression involves the perturbed density distribution. The condition of neutrality is used in determining this distribution since it forces the electron motion to be governed by the positive ions whose velocities and mass are similar to that of the neutral particles. This will be discussed in the second part of the paper where expressions for the distribution are found. In the third part numerical results for a specific sphere velocity and altitude are presented.

1. The Scattering Integral

The radiation field of each electron yields a backscattered power per unit solid angle per electron for unit incident power density given by

$$\sigma_e = \left[e^2 / (4\pi \epsilon_o mc^2) \right]^2 .$$

Here e is the charge on the electron, m its mass, ϵ_o the permittivity of free space, c the velocity of light and MKSC units are to be used. The incident power is given by $PG/(4\pi r^2)$ where P is the total power emitted from the radar antenna, G the antenna gain and r the distance from antenna to electron. The effective collecting area of the antenna is $G \lambda^2/(4\pi)$ so that the scattered power per electron received by the radar for large r is

$$S_e = \frac{PG^2 \lambda^2 \sigma_e}{16\pi^2 r^4} .$$

We now assume the radar is well out of the ionized region of interest so that r is always large. Then the net power received from this region is

$$S = \frac{\lambda^2 \sigma_e P}{16\pi^2} \left| \int \frac{G}{r^2} e^{2ikr} N dv \right|^2 ,$$

where dv is a volume element. For simplicity a beam width wide enough to be essentially constant over the disturbance is assumed, and the slowly varying factor r^{-2} replaced by the range R_o to the sphere and removed from under the integral sign. Finally N is referred to the constant n by writing N = (N-n) + n. The integral of n e^{2ikr} vanishes except for contributions at the "edges" of the region of integration. Of course the distribution n extends beyond the beamwidth of the radar and thus we know these "edges" are not physically significant. They may be neglected with the result that the desired quantity, the net power received due to the disturbance of the density distribution is given by

$$S_D \sim \frac{\lambda^2 \sigma_e PG^2}{16\pi^2 R_o^4} \left| \int e^{2ikr} (N - n) \, dv \right|^2 .$$

The integration is to be extended over the region of interest. In general this will include the entire region over which N-n differs appreciably from zero. However, one might also be interested in considering separately the effects of the region ahead of the sphere and the region behind it. If these were to act as independent scatterers the average returned power (averaged over all relative phases) would be the sum of two expressions S_{D_1} and S_{D_2} corresponding to S_D with the integration in S_{D_1} over the region ahead of the sphere and the region in S_{D_2} over the region behind the sphere.

To put the integral in S in a form suitable for computation it is convenient to refer to Figure 1. The density N must be symmetric about z so that it is convenient to use cylindrical coordinates $\rho, \psi,$ z in the integration. Furthermore one can simplify the integral by using in the expression for $r(\rho)$

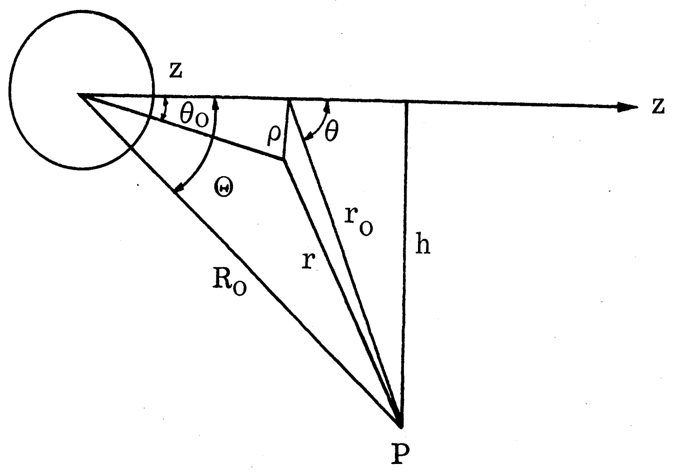

Figure 1.

$$\bar{r}(\rho) = \bar{r}_o - \bar{\rho}; \quad r^2 = r_o^2 + \rho^2 - 2\bar{r}\cdot\bar{\rho}$$

the fact that $\frac{\rho}{r_o} \ll 1$, so that

$$r = r_o \left[1 + \frac{\rho^2}{r_o^2} - \frac{2\rho}{r_o} \sin\theta \cos(\phi - \psi) \right]^{1/2}$$

$$\sim r_o - \rho \sin\theta \cos(\phi - \psi) + \frac{1}{2}\frac{\rho^2}{r_o} - \frac{1}{8}\frac{\rho^2}{r_o} \sin^2\theta \cos^2(\phi - \psi) + \dots$$

In turn r_o is approximated by

$$r_o \simeq R_o + \frac{z^2}{2R_o} - 2z\cos\Theta - \frac{1}{8}\frac{z^2}{R_o}\cos^2\Theta + \dots$$

We shall be interested in $60^0 < \Theta < 120^0$ and hence will neglect the last term as well as those of higher order in z/R_o. Then

$$S = \frac{\lambda^2 \sigma_e PG^2}{16\pi^2 R_o^4} \left| \int_0^{2\pi} d\psi \int_{-\infty}^{\infty} dz \int_0^{\infty} \rho \, d\rho \left[N(\rho, z) - n \right] e^{2ikr(\rho, \psi, z)} \right|^2$$

$$\simeq \frac{\lambda^2 \sigma_e PG^2}{4R_o^4} \left| \int_{-\infty}^{\infty} dz \cdot \exp\left[2ik \left(\frac{z^2}{2R_o} - z\cos\theta\right)\right] \left\{ \int_0^{\infty} \rho \, d\rho \left[N(\rho,z)-n\right] J_o\left[2k\rho\sin\theta(z)\right] \right\} \right|^2$$

The term $\frac{1}{2}\frac{\rho^2}{r_o}$ is neglected in the phase since it will appreciably affect the phase only if $\Theta = 90^0$ and then only where ρ exceeds $\sim .1\sqrt{R_o}$. For such large ρ's the amplitude N-n is negligible. This is not quite true for corresponding values of z. In this consideration we have assumed $k < \sim 20 \text{ m}^{-1}$. Note that in this integral $\sin\theta(z) = R_o \sin\Theta / r_o(z)$.

2. Computation of the Electron Distribution

The steady-state problem of a point charge moving through a fully ionized medium of sufficiently low density has been treated by Kraus and Watson [2]. Their work was extended to the case where a constant magnetic field is present by Greifinger [3]. A good deal of insight into the physical meaning of the above theories which started from the linearized Landau-Vaslov equation was provided by the report of Pappert [4]. In this report Pappert deduced the results of Kraus and Watson from the random phase approximation of Bohm and Pines [5] and also demonstrated the equivalence of these methods to the linearization of the equations of motion and continuity for the ions and electrons under the assumption that an isothermal state exists.+

The problem of an object of finite size has been approached by using the expression obtained in 1950 by C. S. Wang Chang [6]. Chang obtained the zero'th order velocity distribution function for a sphere of radius R at rest in a neutral gas with a streaming velocity V under the assumption that the sphere was sufficiently small and the gas sufficiently dilute that the collisions between the main stream particles and those reflected from the sphere could be neglected. The distribution function so determined satisfies:

+An alternate and simpler derivation of a more general version of the uncoupled microscopic equations of Kraus, Watson and Pappert has been worked out by C. L. Dolph and is given in an Appendix.

(A) The collision-free Boltzmann transport equation in the absence of external forces;

(B) A boundary condition on the surface of the sphere that implies that the sphere neither absorbs nor emits gas particles by itself so that all particles that hit the sphere are re-emitted;

(C) The property that it reduces to the Maxwell-Boltzmann distribution around the streaming velocity at infinity independent of angle.

In addition, this distribution allows for arbitrary amounts of diffuse or specular reflection at the spherical surface. Since the region of interest here involves velocities of the sphere much greater than that of the ions and at the same time much smaller than that of the electrons and altitudes where the mean free paths are large compared to the expected dimensions of the disturbed area, Chang's distribution may be used to provide an order of magnitude estimate of the electron distribution around the sphere when it is assumed that the charge on the sphere is so small that it can be ignored so that the ions will (to all intents and purposes) behave as neutral particles as far as their interaction with the sphere is concerned. The strong coulomb forces should provide electrical neutrality which will then force the electrons to assume a distribution identical in form to Chang's in which only the mass and velocity parameters can be different.

This use of electrical neutrality, while appropriate in ionospheric physics, is less exact than the assumptions usually used in physics of confined plasmas where [7] it is more customary to assume electrical neutrality except for consideration of Poisson's equation while here we ignore any deviations from neutrality in this equation as well. While it would be more exact to assume the Chang distribution as the first term in a perturbation procedure for the Landau-Vaslov equations, it is unlikely that such a refined analysis would affect the radar cross section results+. Other approaches such as that used by Bernstein and Rabinowitz [9] in their discussion of spherical probes would seem to encounter even more intractable analytical difficulties were the Chang distribution to be used in place of the mono-energetic one used by them.

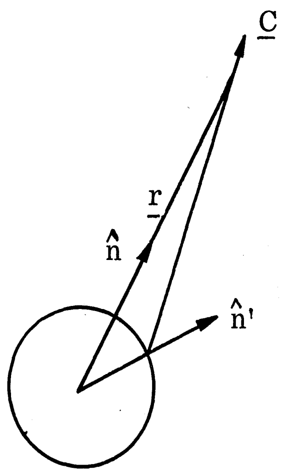

Figure 2.

+Actually the indicated procedure for the second approximation is presently under investigation under another contract for a different purpose. Preliminary analysis seems to indicate the existence of oscillatory solutions for the electron density with frequencies of the order of those characteristic for plasmas modified by an increment dependent upon electron temperature and form factors appropriate to the geometry. See Reference 8.

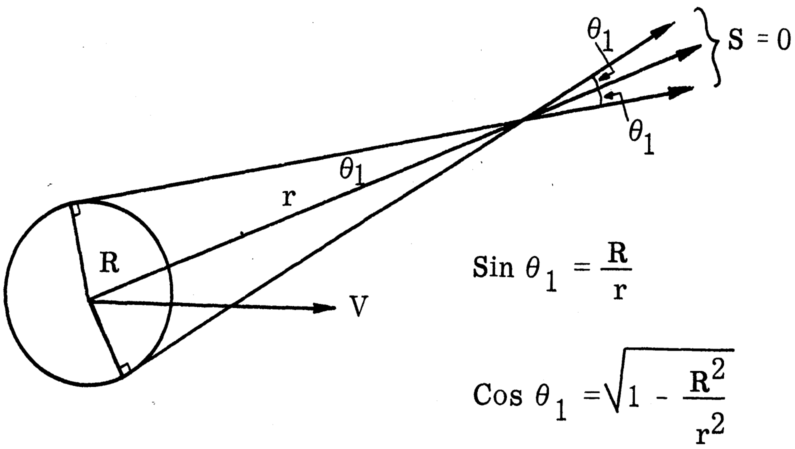

Figure 3.

The zero'th order velocity distribution obtained by Chang is expressed in terms of the following variables.

$\underline{V}'$ = the velocity of the main stream

R = the radius of the sphere

$\underline{r}$ = the point under consideration, or the point at which the velocity is being calculated

$\hat{n}$ = the outward normal to the sphere which passes through the point; $\underline{r} = r\,\hat{n}$ if the center of the sphere is taken as the origin of the coordinate system

$\underline{C}'$ = the velocity vector of gas particles

α = the fraction of molecules that is diffusely reflected from the sphere

$1-\alpha$ = the fraction of molecules that is specularly reflected from the sphere

$\underline{V} = \underline{V}' / \sqrt{2kt/m}$, non-dimensional streaming velocity

$\underline{C} = \underline{C}' / \sqrt{2kt/m}$, non-dimensional velocity vector

$\hat{n}'$ = the normal to the sphere at the point from which the molecules arriving at r with velocity $\underline{C}$ originated. From Figure 2 it is found that

$$\hat{n}' = \frac{\underline{r}}{R} - \frac{\underline{r} \cdot \underline{C}}{RC^2} \underline{C} + r \sqrt{\frac{(\underline{r} \cdot \underline{C})^2}{r^2 C^2} - (1 - \frac{R^2}{r^2})} \frac{\underline{C}}{RC}$$

$\hat{n}_C$ = unit vector in the direction of $\underline{C}$

n = the number of particles present in the unperturbed state

$$\text{erfc}\,(x) = \frac{2}{\sqrt{\pi}} \int_x^{\infty} e^{-t^2} dt = 1 - \text{erf}\,(x)$$

S = $S(x, y, z, \hat{n}_C)$, a discontinuous function which is zero if the particles of velocity $\underline{C}$ at point $\underline{r}(y, x, z)$ come from the sphere and which is one otherwise. That is, S = 0 if $\hat{n}_C$ points away from the sphere and lies in the solid angle subtended by the sphere at the point under consideration.

The distribution can be written as

$$f(\alpha) = \frac{n}{\pi^{3/2}} \Bigg\{ S e^{-(\underline{C} - \underline{V})^2} + \alpha \left[e^{-(\underline{V} \cdot \hat{n}')^2} - \sqrt{\pi} (\underline{V} \cdot \hat{n}') \,\text{erfc}\, (\underline{V} \cdot \hat{n}') \right] (1 - S) e^{-C^2}$$

$$+ (1 - \alpha)(1 - S) e^{-\left[\underline{C} - \underline{V} - 2\hat{n}' (\hat{n}' \cdot \underline{C})\right]^2} \Bigg\}$$

The function S which is described above can be represented analytically as

$$S = \frac{1}{2}\,(1 - \mathrm{sign}(\hat{n}\cdot\underline{C}) + \left[\frac{1}{4}\,(1 + \mathrm{sign}(\hat{n}\cdot\underline{C})\right]\left[1 + \mathrm{sign}\left\{(1 - \frac{R^2}{r^2})^{1/2} - \frac{\hat{n}\cdot\underline{C}}{C}\right\}\right]\hat{n}$$

and it has the properties that for r approaching infinity, S approaches 1, while for r approaching the sphere **R**,

$$S = \frac{1}{2}\,(1 - \mathrm{sign}\ \hat{n}\cdot\underline{C}).$$

Furthermore, if θ is the angle between $\underline{r}$ and $\underline{C}$ then, as can be seen from Figure 3,

$$S = 0 \text{ if } 1 \geqslant \cos\theta \geqslant (1 - \frac{R^2}{r^2})^{1/2} = \cos\theta_1$$

$$S = 1 \text{ if } \cos\theta < \cos\theta_1 .$$

The Density Distribution for Ions and Electrons in the Neighborhood of the Sphere for the Case of Diffuse Reflection

The necessary calculations are considerably simplified if it is assumed that only diffuse reflection occurs so that α may be set equal to unity. Fortunately this appears to be a good approximation to the physical situation [6], [10], [11].

We shall therefore calculate

$$\int f(1)\, d^3 C$$

and take up the two terms separately, treating first the contribution

$$I_1 = \frac{n}{\pi^{3/2}} \int S\, e^{-(\underline{C} - \underline{V})^2} dV$$

from the main stream. To evaluate I_1 we determine S in rectangular C space C_x, C_y, C_z. For convenience set $\hat{n}$ in the direction of C_z.

If

$$\left(1 - \frac{R^2}{r^2}\right)^{1/2} - \frac{C_z}{\left(C_x^2 + C_y^2 + C_z^2\right)^{1/2}} < 0$$

then $C_z > 0$ and

$$S = \frac{1}{2}\left[1 - \text{sign}\ C_z\right] = 0,\ C_z > 0.$$

Also, for all $\underline{C}$ for which

$$\left(1 - \frac{R^2}{r^2}\right)^{1/2} - \frac{C_z}{\left(C_x^2 + C_y^2 + C_z^2\right)^{1/2}} > 0,$$

S = 1. Since both sides of the first inequality are positive it may be squared and solved for C_z. The result is

$$C_z > \left(\frac{r^2}{R^2} - 1\right)^{1/2} \left(C_x^{\,2} + C_y^{\,2}\right)^{1/2} \equiv C_{z_o},$$

so that if $C_z \geqslant C_{z_o}$, $S = 0$. Similarly if $C_z < C_{z_o}$, $S = 1$.

Thus we must evaluate

$$I_1 = \frac{n}{\pi^{3/2}} \int_{-\infty}^{\infty} dC_x \int_{-\infty}^{\infty} dC_y \int_{-\infty}^{C_{z_o}} dC_z \cdot e^{-\left[(C_x - V_x)^2 + (C_y - V_y)^2 + (C_z - V_z)^2\right]}.$$

The C_z integral is

$$\int_{-\infty}^{C_{z_o}} e^{-(C_z - V_z)^2} dC_z = \int_{-\infty}^{C_{z_o} - V_z} e^{-t^2} dt = \frac{\sqrt{\pi}}{2} \left[\mathrm{erf}\,(C_{z_o} - V_z) + 1\right].$$

Hence

$$I_1 = \frac{n}{2} + \frac{n}{2\pi} \int_{-\infty}^{\infty} \int_{-\infty}^{\infty} e^{-\left[(C_x - V_x)^2 + (C_y - V_y)^2\right]} \mathrm{erf}(C_{z_o} - V)\, dC_x\, dC_y.$$

Introduce polar coordinates as follows:

$$C_x = \rho \cos \phi \qquad V_x = \sqrt{V^2 - V_z^{\,2}} \cos \psi$$

$$C_y = \rho \sin \phi \qquad V_y = \sqrt{V^2 - V_z^{\,2}} \sin \psi.$$

Then

$$I_1 = \frac{n}{2}\left\{1 + \frac{1}{\pi}\, e^{-(V^2-V_z^2)} \int_0^{\infty} d\rho\, \rho\, e^{-\rho^2}\, \operatorname{erf}\left(\rho\sqrt{\frac{r^2}{R^2}-1} - V_z\right)\cdot\right.$$

$$\left.\cdot \int_0^{2\pi} e^{2\rho\sqrt{V^2-V_z^2}\cos(\phi-\psi)}\, d\phi\right\}$$

$$= \frac{n}{2}\left\{1 + 2e^{-(V^2-V_z^2)} \int_0^{\infty} d\rho\, \rho\, e^{-\rho^2}\, \operatorname{erf}\left(\rho\sqrt{\frac{r^2}{R^2}-1} - V_z\right) I_o\left(2\rho\sqrt{V^2-V_z^2}\right)\right\}$$

where $I_o(\,)$ is the Bessel function of imaginary argument and zero order, and

$$V_z = \overline{V}\cdot\hat{n} = V\cos\theta_o$$

$$V^2 - V_z^2 = V^2\sin^2\theta\,.$$

Hence

$$I_1 = \frac{n}{2}\left\{1 + 2e^{-V^2\sin^2\theta_o} \int_0^{\infty} d\rho\, \rho\, e^{-\rho^2}\, \operatorname{erf}\left(\rho\sqrt{\frac{r^2}{R^2}-1} - V\cos\theta_o\right) I_o\left(2\rho V\sin\theta_o\right)\right\}.$$

In the limiting case, $r = R$

$$I_1 = \frac{n}{2}\left\{1 + 2e^{-V^2\sin^2\theta_o}\, \operatorname{erf}\left(-V\cos\theta_o\right) \int_0^{\infty} d\rho\, \rho\, e^{-\rho^2}\, I_o\left(2\rho V\sin\theta_o\right)\right\} .$$

To carry out the integration, integrate once by parts to obtain

$$I = \int_0^\infty e^{-\rho^2} \rho\, I_o(2u\rho) = -\frac{1}{2} e^{-\rho^2} \Big|_0^\infty + u \int_0^\infty e^{-\rho^2} I_1(2u\rho)\, d\rho,$$

with $u = V \sin\theta_o$. The integral on the right is given in the Bateman Manuscript Project series [12] leading to the result

$$I = \frac{1}{2} + \frac{\sqrt{\pi}}{2} u\, e^{\frac{u^2}{2}} I_{1/2}\left(\frac{u^2}{2}\right).$$

Since

$$I_{1/2}(z) = \sqrt{\frac{2}{\pi z}} \sinh z$$

one gets

$$I = \frac{1}{2} e^{u^2},$$

and hence for $r = R$,

$$I_1 = \frac{n}{2} \left\{ 1 + \operatorname{erf}(-V \cos\theta_o) \right\} = \frac{n}{2} \operatorname{erfc}(V \cos\theta_o).$$

This checks the direct integration of I_1 for r set equal to **R** in advance, since in this case, $S = 1$ only if $C_x \leqslant 0$.

When $r \longrightarrow \infty$,

$$\operatorname{erf}\left(\rho \sqrt{\frac{r^2}{R^2} - 1} - V_z\right) \longrightarrow \operatorname{erf}(\infty) = 1$$

and one obtains

$$I_1 \longrightarrow \frac{n}{2} \left\{ 1+1 \right\} = n$$

as one should.

For the two cases of $\theta_o = 0$ and $\theta_o = \pi$ the quantity I_1 can be evaluated exactly if spherical coordinates are used. If one uses r as axis

$$\underline{r} = r(0, 0, 1)$$

$$\underline{V} = V(\sin\theta_o \cos\phi_o, \sin\theta_o \sin\phi_o, \cos\theta_o)$$

$$\underline{C} = C(\sin\theta \cos\phi, \sin\theta \sin\phi, \cos\theta)$$

and

$$I_1 = \frac{n}{\pi^{3/2}} \int_0^\infty C^2\, dc \int_0^{2\pi} d\phi \int_0^{\theta_1} \sin\theta$$

$$\exp\left\{ -(C^2+V^2)+2CV\left[\cos\theta \cos\theta_o + \sin\theta \sin\theta_o (\cos\phi - \phi_o)\right] \right\} d\theta .$$

By straightforward integration of this form of I_1 when $\theta_o = 0$ one finds

$$I_1(0) = \frac{n}{2} \left\{ \operatorname{erfc} V + e^{-V^2 \sin^2\theta_1} \cos\theta_1 \operatorname{erfc}(-V\cos\theta_1) \right\}$$

$$= \frac{n}{2} \left\{ \operatorname{erfc} V + \sqrt{1 - \frac{R^2}{r^2}}\; e^{-V^2 \frac{R^2}{r^2}} \operatorname{erfc}\left(-V \sqrt{1 - \frac{R^2}{r^2}} \right) \right\} .$$

A similar discussion for $\theta_o = \pi$ leads to the value

$$I_1(\pi) = \frac{n}{2}\left\{ \text{erfc}(-V) + \sqrt{1 - \frac{R^2}{r^2}}\; e^{-V^2 \frac{R^2}{r^2}} \text{erfc}\left(V\sqrt{1 - \frac{R^2}{r^2}}\right)\right\}.$$

For $r = R$ both of these reduce to our previously obtained approximation since the additional term is zero there. Likewise in the limit as $r \rightarrow \infty$, we obtain the free stream density as we should. For either $\theta = 0$ or $\theta = \pi$ the above reduces to

$$\lim_{r \rightarrow \infty} I_1 = \frac{n}{2}\left[\text{erfc}(V) + \text{erfc}(-V)\right] = n$$

which is correct.

To evaluate the term containing the effect of the diffusely reflected particles, it is necessary to consider the integral

$$I_2 = \frac{n}{\pi^{3/2}} \int d^3 \underline{C} \left\{ e^{-(\underline{V}\cdot\hat{n}')^2} - \sqrt{\pi}(\underline{V}\cdot\hat{n}')\,\text{erfc}(\underline{V}\cdot\hat{n}')\right\} (1-S)\, e^{-C^2}.$$

Introducing r as the polar axis again so that

$$\begin{aligned}\hat{n}' = \; & \left[(-\cos\theta)\, r/R + r/R\sqrt{\cos^2\theta - (1 - R^2/r^2)}\right] \sin\theta \cos\phi, \\ & \left[(-\cos\theta)\, r/R + r/R\sqrt{\cos^2\theta - (1 - R^2/r^2)}\right] \sin\theta \sin\phi, \\ & (r/R)\left[(-r\cos\theta)/R + r/R\sqrt{\cos^2\theta - (1 - R^2/r^2)}\right] \cos\theta\end{aligned}$$

leads to

$$\underline{V}\cdot\hat{n}' = \frac{Vr}{R}\Bigg\{\cos\theta_o$$

$$-\left[\cos\theta - \sqrt{\cos^2\theta - (1-R^2/r^2)}\right]\left[\cos\theta\cos\theta_o + \sin\theta\sin\theta_o\cos(\phi-\phi_o)\right]\Bigg\}$$

so that I_2 is quite intractable without approximation. However, as mentioned earlier $(1-S) = 1$ if and only if

$$0 \leqslant \theta \leqslant \theta_1 = \arccos\left(1 - \frac{R^2}{r^2}\right)^{1/2}$$

and in this range

$$\cos\theta - \sqrt{\cos^2\theta - \left(1 - \frac{R^2}{r^2}\right)}$$

is a very slowly varying function which has extremes at $\theta = 0$, and $\theta = \theta_1$ with values $(1 - R/r)$ and $\sqrt{1 - \frac{R^2}{r^2}}$ respectively. We will therefore replace the complicated expression for $(\underline{V}\cdot\hat{n}')$ in $\exp -(\underline{V}\cdot\hat{n}')$ and $\mathrm{erfc}(\underline{V}\cdot\hat{n}')$ by its first term

$$\underline{V}\cdot\hat{n}' \cong Vr\frac{\cos\theta_o}{R} .$$

The integral I_2 is therefore evaluated as

$$I_2 \cong I_2^A = \frac{n}{\pi^{3/2}}\int_0^\infty e^{-C^2}C^2\,dC\int_0^{2\pi}d\phi\int_{\theta=0}^{\theta_1}\sin\theta\,d\theta\Bigg\{e^{-\frac{V^2r^2}{R^2}\cos^2\theta_o}$$

$$-\sqrt{\pi}(\underline{V}\cdot\hat{n}')\,\mathrm{erfc}\left(\frac{Vr\cos\theta_o}{R}\right)\Bigg\}$$

where the full expression for $(\underline{V} \cdot \hat{n}')$ is used where it appears explicitly. Straightforward integration then yields the following expression for I_2^A

$$I_2^A = \frac{n}{2}\left[-\cos\theta\right]_0^{\theta_1} e^{-\frac{V^2 r^2}{R^2}\cos^2\theta_o}$$

$$-\frac{n}{4\pi}\int_0^{2\pi}\sqrt{\pi}\,\mathrm{erfc}\left(\frac{Vr}{R}\cos\theta_o\right)\int_0^{\theta_1}(V.n')\sin\theta\, d\theta\, d\phi$$

$$= \frac{n}{2}\left[1-\sqrt{1-\frac{R^2}{r^2}}\right] e^{-\frac{V^2 r^2}{R^2}\cos^2\theta_o} - \frac{n}{2}\sqrt{\pi}\,\mathrm{erfc}\left(\frac{Vr}{R}\cos\theta_o\right) I_3$$

where

$$I_3 = \int_0^{2\pi}\int_0^{\theta_1}(V\cdot n')\sin\theta\; d\theta\; d\phi$$

$$= 2\pi\int_0^{\theta_1}\frac{Vr}{R}\left\{\cos\theta_o - \left[\cos\theta - \sqrt{\cos^2\theta - (1-\frac{R^2}{r^2})}\right]\cos\theta\;\cos\theta_o\right\}\sin\theta\; d\theta$$

$$= 2\pi\,\frac{Vr}{R}\cos\theta_o\left\{1-\sqrt{1-\frac{R^2}{r^2}} + \frac{1}{3}\,\frac{R^3}{r^3} - \frac{1}{3}\left[1-(1-\frac{R^2}{r^2})^{3/2}\right]\right\}.$$

The approximation of I_2 by I_2^A is poorest in intermediate ranges of r and hence it is of interest to have an upper bound in this region. The difference between I_2^A and I_2 is bounded above by

$$\left[e^{-(\frac{Vr}{R})^2 (\cos\theta_o + \sqrt{1 - \frac{R^2}{r^2}})^2} - e^{-(\frac{Vr}{R})^2 \cos^2\theta_o} \right] \cdot \left(1 - \sqrt{1 - \frac{R^2}{r^2}} \right)$$

$$+ \sqrt{\pi} \left(\frac{Vr}{R} \right)^2 \sqrt{1 - \frac{R^2}{r^2}} \cos\theta_o \, e^{-(\frac{Vr}{R})^2 (\cos\theta_o + \sqrt{1 - \frac{R^2}{r^2}})^2}$$

$$\left\{ 1 - \sqrt{1 - \frac{R^2}{r^2}} + \frac{1}{3} \frac{R^3}{r^3} - \frac{1}{3} \left[1 - (1 - \frac{R^2}{r^2})^{3/2} \right] \right\},$$

for all r and θ_o such that $\sqrt{1 - \frac{R^2}{r^2}} < 2 \left| \cos\theta_o \right|$. The plus sign is to be used for $\cos\theta_o < 0$ and the minus sign for $\cos\theta_o > 0$.

3. Numerical Results for Electron Density Distribution and Radar Cross Sections

The formulas of Part 2 were applied to a typical [7] case of interest for which V = 5. This corresponds, for example, to a satellite altitude of 500 km and speed V' = 8 km/sec. Curves of constant relative density N/n are presented in Figures 4 and 5. They clearly show the build-up of density ahead of the sphere and the "hole" developed in the rear. The ion deficiency in the rear extends to about 50 sphere radii.

More detailed data for N on the sphere and along the positive z axis (behind the sphere) is given in Table I and Table II. Table I was computed on a desk calculator using the exact formulas for R=r or $\theta_o=0$, pp 16, 17. Table II was computed by numerical integration on an IBM 704 of the integral on page 15. The integration steps were not small enough to get a good check on the exact results for $\rho = 0$, $1 < z < 2.5$.

Radar cross sections (4π times differential cross sections) were computed from the formula

$$\sigma = 4\pi \sigma_e n^2 \left| \int_V \left(\frac{N}{n} - 1 \right) e^{2ikr} dv \right|^2$$

according to the development in Part 1. For electrons $4\pi \sigma_e \sim 10^{-28} m^2$. A value of $n = 10^{12}$ electrons/m^3 is used for the electron density at 500 km altitude and the resulting values of σ are given in Table II for a sphere of 1m radius. Three aspect angles Θ (see Figure 1) and three wavelengths, λ = 15, 6.3, and 1

Table I

$$\text{Density Ratio} = \frac{\text{Density}}{\text{Free Stream Density}} = \frac{N}{n}$$

On Sphere, r = R | Behind Sphere at 0^o

θ	N/n	z	N/n
0^o	9.0×10^{-13}	1	9.0×10^{-13}
5^o	1.0923×10^{-12}	2	1.6718×10^{-3}
10^o	1.9443×10^{-12}	3	5.8621×10^{-2}
15^o	4.9876×10^{-12}	4	2.0296×10^{-1}
20^o	1.7947×10^{-11}	5	3.6045×10^{-1}
25^o	8.7137×10^{-11}	6	4.9237×10^{-1}
30^o	5.4587×10^{-10}	7	5.9422×10^{-1}
35^o	4.1834×10^{-9}	8	6.7133×10^{-1}
40^o	3.6932×10^{-8}	8.5	7.0258×10^{-1}
45^o	3.5343×10^{-7}	9	7.2990×10^{-1}
50^o	3.4398×10^{-6}	9.5	7.5384×10^{-1}
55^o	3.1943×10^{-5}	10	7.7490×10^{-1}
60^o	2.6707×10^{-4}	20	9.3824×10^{-1}
65^o	1.9583×10^{-3}	30	9.7206×10^{-1}
70^o	1.1018×10^{-2}	40	9.8419×10^{-1}
75^o	5.0194×10^{-2}	50	9.8985×10^{-1}
80^o	1.7613×10^{-1}		
85^o	4.7471×10^{-1}		
86^o	5.6145×10^{-1}		
87^o	6.5761×10^{-1}		
88^o	7.6306×10^{-1}		
89^o	8.7739×10^{-1}		
90^o	1.0		

Table II

Table of N(ρ, z) used in Numerical Integration

RHO \ Z	0.	-0.5	-1.0	-1.5	-2.0	-2.5	-3.0	-3.5	-4.0	-4.5	-5.0
0.			9.862	3.102	2.042	1.623	1.413	1.294	1.220	1.171	1.136
0.100			8.939	3.085	2.038	1.621	1.413	1.294	1.220	1.170	1.136
0.200			7.978	3.037	2.025	1.616	1.410	1.293	1.219	1.170	1.136
0.300			7.027	2.961	2.004	1.608	1.407	1.291	1.218	1.169	1.135
0.400			6.133	2.861	1.976	1.597	1.402	1.288	1.216	1.168	1.135
0.500			5.323	2.746	1.942	1.584	1.396	1.285	1.215	1.167	1.134
0.600			4.613	2.619	1.903	1.568	1.388	1.281	1.212	1.166	1.133
0.700			4.007	2.488	1.859	1.550	1.380	1.276	1.210	1.164	1.132
0.800			3.499	2.357	1.814	1.531	1.370	1.271	1.207	1.162	1.131
0.900		4.273	3.077	2.230	1.767	1.510	1.360	1.266	1.203	1.160	1.129
1.000	1.000	3.161	2.730	2.110	1.719	1.489	1.349	1.260	1.200	1.158	1.128
1.100	1.290	2.565	2.446	1.998	1.672	1.467	1.338	1.253	1.196	1.156	1.126
1.200	1.223	2.239	2.214	1.895	1.626	1.444	1.326	1.246	1.192	1.153	1.125
1.300	1.180	1.914	2.024	1.802	1.581	1.422	1.314	1.239	1.188	1.150	1.123
1.400	1.149	1.723	1.868	1.718	1.538	1.400	1.301	1.232	1.183	1.147	1.121
1.500	1.127	1.582	1.740	1.642	1.498	1.378	1.289	1.225	1.179	1.144	1.119
1.600	1.109	1.475	1.634	1.575	1.460	1.357	1.277	1.217	1.174	1.141	1.117
1.700	1.095	1.371	1.546	1.515	1.425	1.336	1.264	1.210	1.169	1.138	1.115
1.800	1.084	1.327	1.473	1.462	1.392	1.316	1.252	1.203	1.164	1.135	1.112
1.900	1.074	1.276	1.411	1.415	1.361	1.297	1.241	1.195	1.159	1.132	1.110
2.000	1.066	1.211	1.359	1.374	1.333	1.279	1.229	1.188	1.155	1.128	1.108
2.100	1.060	1.202	1.315	1.337	1.307	1.262	1.218	1.180	1.150	1.125	1.105
2.200	1.054	1.174	1.278	1.304	1.284	1.246	1.208	1.173	1.145	1.122	1.103
2.300	1.028	1.151	1.246	1.275	1.262	1.231	1.197	1.166	1.140	1.118	1.101
2.400	1.045	1.126	1.219	1.249	1.242	1.217	1.187	1.160	1.135	1.115	1.098
2.500	1.041	1.116	1.195	1.227	1.224	1.203	1.178	1.153	1.131	1.112	1.096
2.600	1.038	1.103	1.175	1.206	1.207	1.191	1.169	1.146	1.126	1.108	1.094
2.700	1.035	1.091	1.157	1.188	1.191	1.179	1.160	1.140	1.122	1.105	1.091
2.800	1.032	1.081	1.142	1.172	1.177	1.168	1.152	1.134	1.117	1.102	1.089
2.900	1.030	1.073	1.128	1.157	1.165	1.158	1.144	1.128	1.113	1.099	1.086
3.000	1.028	1.065	1.116	1.144	1.153	1.148	1.137	1.123	1.109	1.096	1.084
3.100	1.026	1.059	1.106	1.133	1.143	1.140	1.130	1.118	1.105	1.093	1.082
3.200	1.024	1.053	1.096	1.122	1.132	1.131	1.123	1.112	1.101	1.090	1.080
3.300	1.023	1.049	1.088	1.113	1.124	1.123	1.117	1.108	1.097	1.087	1.077
3.400	1.021	1.044	1.080	1.104	1.115	1.116	1.111	1.103	1.093	1.084	1.075
3.500	1.020	1.040	1.074	1.097	1.108	1.109	1.106	1.098	1.090	1.081	1.073
3.600	1.019	1.037	1.068	1.089	1.100	1.103	1.100	1.094	1.086	1.078	1.071
3.700	1.018	1.034	1.063	1.083	1.094	1.097	1.095	1.090	1.083	1.076	1.069
3.800	1.017	1.031	1.058	1.077	1.088	1.092	1.090	1.086	1.080	1.073	1.067
3.900	1.016	1.029	1.054	1.072	1.082	1.087	1.086	1.082	1.077	1.071	1.065
4.000	1.015	1.026	1.049	1.067	1.077	1.082	1.082	1.079	1.074	1.068	1.063
4.100	1.014	1.024	1.046	1.062	1.073	1.077	1.078	1.075	1.071	1.066	1.061
4.200	1.014	1.022	1.043	1.058	1.068	1.073	1.074	1.072	1.068	1.064	1.059
4.300	1.013	1.021	1.040	1.055	1.064	1.069	1.070	1.069	1.066	1.062	1.057
4.400	1.012	1.019	1.037	1.051	1.060	1.065	1.067	1.066	1.063	1.060	1.056
4.500	1.012	1.018	1.035	1.048	1.057	1.062	1.064	1.063	1.061	1.058	1.054
4.600	1.011	1.017	1.032	1.045	1.054	1.059	1.061	1.060	1.059	1.056	1.052
4.700	1.011	1.016	1.030	1.042	1.051	1.056	1.058	1.058	1.056	1.054	1.051
4.800	1.010	1.015	1.028	1.040	1.048	1.053	1.055	1.056	1.054	1.052	1.049
4.900	1.010	1.014	1.027	1.037	1.045	1.050	1.053	1.053	1.052	1.050	1.048
5.000	1.009	1.013	1.025	1.035	1.043	1.048	1.050	1.051	1.050	1.048	1.046

Table II (continued)

Table of $N(\rho, z)$ used in Numerical Integration

RHO \ Z	0.	0.5	1.0	1.5	2.0	2.5	3.0	3.5	4.0	4.5
0.			0.001	0.001	0.025	0.018	0.059	0.125	0.204	0.284
0.100			0.001	0.001	0.030	0.020	0.064	0.130	0.209	0.289
0.200			0.000	0.001	0.051	0.028	0.078	0.146	0.224	0.302
0.300			0.000	0.001	0.011	0.045	0.102	0.173	0.249	0.324
0.400			0.000	0.002	0.024	0.073	0.138	0.211	0.284	0.354
0.500			0.000	0.009	0.050	0.115	0.187	0.259	0.327	0.391
0.600			0.001	0.030	0.099	0.176	0.250	0.317	0.378	0.434
0.700			0.009	0.085	0.177	0.257	0.324	0.382	0.434	0.482
0.800			0.068	0.192	0.285	0.354	0.408	0.454	0.495	0.533
0.900		0.032	0.250	0.355	0.417	0.462	0.498	0.529	0.558	0.585
1.000	1.000	0.514	0.528	0.543	0.557	0.572	0.587	0.603	0.620	0.637
1.100	1.290	0.892	0.772	0.715	0.688	0.676	0.672	0.674	0.680	0.688
1.200	1.223	0.984	0.912	0.842	0.795	0.766	0.749	0.739	0.735	0.736
1.300	1.180	0.998	0.971	0.922	0.875	0.839	0.814	0.797	0.786	0.780
1.400	1.150	1.000	0.991	0.964	0.928	0.894	0.866	0.845	0.830	0.820
1.500	1.127	1.000	0.997	0.985	0.961	0.933	0.907	0.885	0.868	0.855
1.600	1.110	1.000	0.999	0.994	0.979	0.959	0.937	0.917	0.899	0.885
1.700	1.096	1.000	1.000	0.997	0.990	0.976	0.959	0.941	0.924	0.910
1.800	1.084	1.000	1.000	0.998	0.995	0.986	0.973	0.959	0.944	0.930
1.900	1.075	1.000	1.000	1.000	0.997	0.992	0.983	0.972	0.959	0.947
2.000	1.067	1.000	1.000	1.000	0.999	0.996	0.990	0.969	0.971	0.960
2.100	1.060	1.000	1.000	1.000	0.999	0.998	0.994	0.987	0.979	0.970
2.200	1.055	1.000	1.000	1.000	1.000	0.999	0.996	0.992	0.986	0.978
2.300	1.029	1.000	1.000	1.000	1.000	0.978	0.998	0.995	0.990	0.984
2.400	1.045	1.000	1.000	1.000	1.000	1.000	0.999	0.996	0.993	0.988
2.500	1.042	1.000	1.000	1.000	1.000	1.000	0.999	0.970	0.995	0.992
2.600	1.038	1.000	1.000	1.000	1.000	1.000	0.999	0.999	0.997	0.994
2.700	1.035	1.000	1.000	1.000	1.000	1.000	1.000	0.999	0.998	0.996
2.800	1.033	1.000	1.000	1.000	1.000	1.000	1.000	0.999	0.999	0.997
2.900	1.031	1.000	1.000	1.000	1.000	1.000	1.000	1.000	0.999	0.998
3.000	1.028	1.000	1.000	1.000	1.000	1.000	1.000	1.000	0.999	0.999
3.100	1.027	1.000	1.000	1.000	1.000	1.000	1.000	1.000	1.000	0.999
3.200	1.025	1.000	1.000	1.000	1.000	1.000	1.000	1.000	1.000	0.999
3.300	1.024	1.000	1.000	1.000	1.000	1.000	1.000	1.000	1.000	0.999
3.400	1.022	1.000	1.000	1.000	1.000	1.000	1.000	1.000	1.000	1.000
3.500	1.021	1.000	1.000	1.000	1.000	1.000	1.000	1.000	1.000	1.000
3.600	1.020	1.000	1.000	1.000	1.000	1.000	1.000	1.000	1.000	1.000
3.700	1.019	1.000	1.000	1.000	1.000	1.000	1.000	1.000	1.000	1.000
3.800	1.018	1.000	1.000	1.000	1.000	1.000	1.000	1.000	1.000	1.000
3.900	1.017	1.000	1.000	1.000	1.000	1.000	1.000	1.000	1.000	1.000
4.000	1.016	1.000	1.000	1.000	1.000	1.000	1.000	1.000	1.000	1.000
4.100	1.015	1.000	1.000	1.000	1.000	1.000	1.000	1.000	1.000	1.000
4.200	1.014	1.000	1.000	1.000	1.000	1.000	1.000	1.000	1.000	1.000
4.300	1.014	1.000	1.000	1.000	1.000	1.000	1.000	1.000	1.000	1.000
4.400	1.013	1.000	1.000	1.000	1.000	1.000	1.000	1.000	1.000	1.000
4.500	1.012	1.000	1.000	1.000	1.000	1.000	1.000	1.000	1.000	1.000
4.600	1.012	1.000	1.000	1.000	1.000	1.000	1.000	1.000	1.000	1.000
4.700	1.011	1.000	1.000	1.000	1.000	1.000	1.000	1.000	1.000	1.000
4.800	1.011	1.000	1.000	1.000	1.000	1.000	1.000	1.000	1.000	1.000
4.900	1.010	1.000	1.000	1.000	1.000	1.000	1.000	1.000	1.000	1.000
5.000	1.010	1.000	1.000	1.000	1.000	1.000	1.000	1.000	1.000	1.000

Table II (continued)

Table of N(ρ, z) used in Numerical Integration

RHO \ z	5.0	5.5	6.0	6.5	7.0	7.5	8.0	8.5	9.0
0.	0.361	0.431	0.493	0.547	0.595	0.636	0.672	0.703	0.730
0.100	0.365	0.434	0.496	0.549	0.597	0.637	0.673	0.704	0.732
0.200	0.376	0.443	0.503	0.556	0.601	0.641	0.676	0.707	0.735
0.300	0.395	0.459	0.515	0.566	0.610	0.648	0.684	0.711	0.738
0.400	0.420	0.479	0.532	0.579	0.621	0.657	0.692	0.717	0.742
0.500	0.045	0.504	0.553	0.596	0.634	0.668	0.700	0.725	0.749
0.600	0.486	0.534	0.577	0.616	0.651	0.682	0.709	0.734	0.756
0.700	0.526	0.567	0.604	0.638	0.669	0.697	0.722	0.745	0.765
0.800	0.568	0.601	0.633	0.662	0.688	0.713	0.736	0.756	0.775
0.900	0.612	0.638	0.663	0.687	0.709	0.731	0.750	0.768	0.785
1.000	0.656	0.675	0.694	0.713	0.731	0.749	0.766	0.781	0.796
1.100	0.699	0.711	0.725	0.739	0.753	0.767	0.781	0.795	0.807
1.200	0.740	0.746	0.755	0.765	0.775	0.786	0.797	0.809	0.818
1.300	0.778	0.780	0.784	0.790	0.797	0.805	0.814	0.822	0.831
1.400	0.814	0.811	0.811	0.814	0.818	0.823	0.829	0.836	0.843
1.500	0.846	0.840	0.837	0.836	0.838	0.841	0.845	0.850	0.855
1.600	0.873	0.866	0.860	0.858	0.857	0.858	0.860	0.863	0.867
1.700	0.898	0.888	0.882	0.877	0.875	0.874	0.874	0.876	0.819
1.800	0.918	0.908	0.900	0.895	0.891	0.888	0.888	0.888	0.889
1.900	0.935	0.925	0.917	0.910	0.906	0.902	0.900	0.899	0.889
2.000	0.950	0.940	0.932	0.925	0.919	0.915	0.912	0.910	0.909
2.100	0.961	0.952	0.944	0.937	0.931	0.926	0.923	0.920	0.919
2.200	0.970	0.962	0.954	0.947	0.941	0.936	0.932	0.929	0.927
2.300	0.977	0.970	0.963	0.957	0.951	0.946	0.941	0.938	0.935
2.400	0.983	0.977	0.971	0.964	0.959	0.954	0.948	0.946	0.943
2.500	0.987	0.982	0.977	0.971	0.966	0.961	0.956	0.953	0.949
2.600	0.991	0.986	0.981	0.976	0.972	0.967	0.963	0.959	0.956
2.700	0.993	0.990	0.985	0.980	0.977	0.972	0.968	0.964	0.961
2.800	0.995	0.992	0.989	0.985	0.981	0.977	0.973	0.969	0.966
2.900	0.996	0.994	0.991	0.988	0.984	0.981	0.977	0.974	0.971
3.000	0.997	0.995	0.993	0.990	0.987	0.984	0.981	0.978	0.975
3.100	0.998	0.996	0.995	0.992	0.989	0.987	0.984	0.981	0.978
3.200	0.999	0.997	0.996	0.994	0.992	0.989	0.987	0.984	0.981
3.300	0.999	0.998	0.997	0.995	0.993	0.991	0.989	0.986	0.984
3.400	0.999	0.999	0.998	0.996	0.995	0.993	0.991	0.988	0.986
3.500	1.000	0.999	0.998	0.997	0.996	0.994	0.992	0.990	0.988
3.600	1.000	0.999	0.999	0.998	0.997	0.995	0.994	0.992	0.990
3.700	1.000	0.999	0.999	0.998	0.997	0.996	0.995	0.993	0.991
3.800	1.000	0.999	0.999	0.999	0.998	0.997	0.996	0.994	0.993
3.900	1.000	1.000	0.999	0.999	0.998	0.997	0.996	0.995	0.994
4.000	1.000	1.000	0.999	0.999	0.999	0.998	0.997	0.996	0.995
4.100	1.000	1.000	1.000	0.999	0.999	0.998	0.998	0.997	0.995
4.200	1.000	1.000	1.000	0.999	0.999	0.999	0.998	0.997	0.996
4.300	1.000	1.000	1.000	1.000	0.999	0.999	0.998	0.998	0.997
4.400	1.000	1.000	1.000	1.000	0.999	0.999	0.999	0.998	0.997
4.500	1.000	1.000	1.000	1.000	1.000	0.999	0.999	0.998	0.998
4.600	1.000	1.000	1.000	1.000	1.000	0.999	0.999	0.999	0.998
4.700	1.000	1.000	1.000	1.000	1.000	0.999	0.999	0.999	0.999
4.800	1.000	1.000	1.000	1.000	1.000	1.000	0.999	0.999	0.999
4.900	1.000	1.000	1.000	1.000	1.000	1.000	0.999	0.999	0.999
5.000	1.000	1.000	1.000	1.000	1.000	1.000	1.000	1.000	0.999

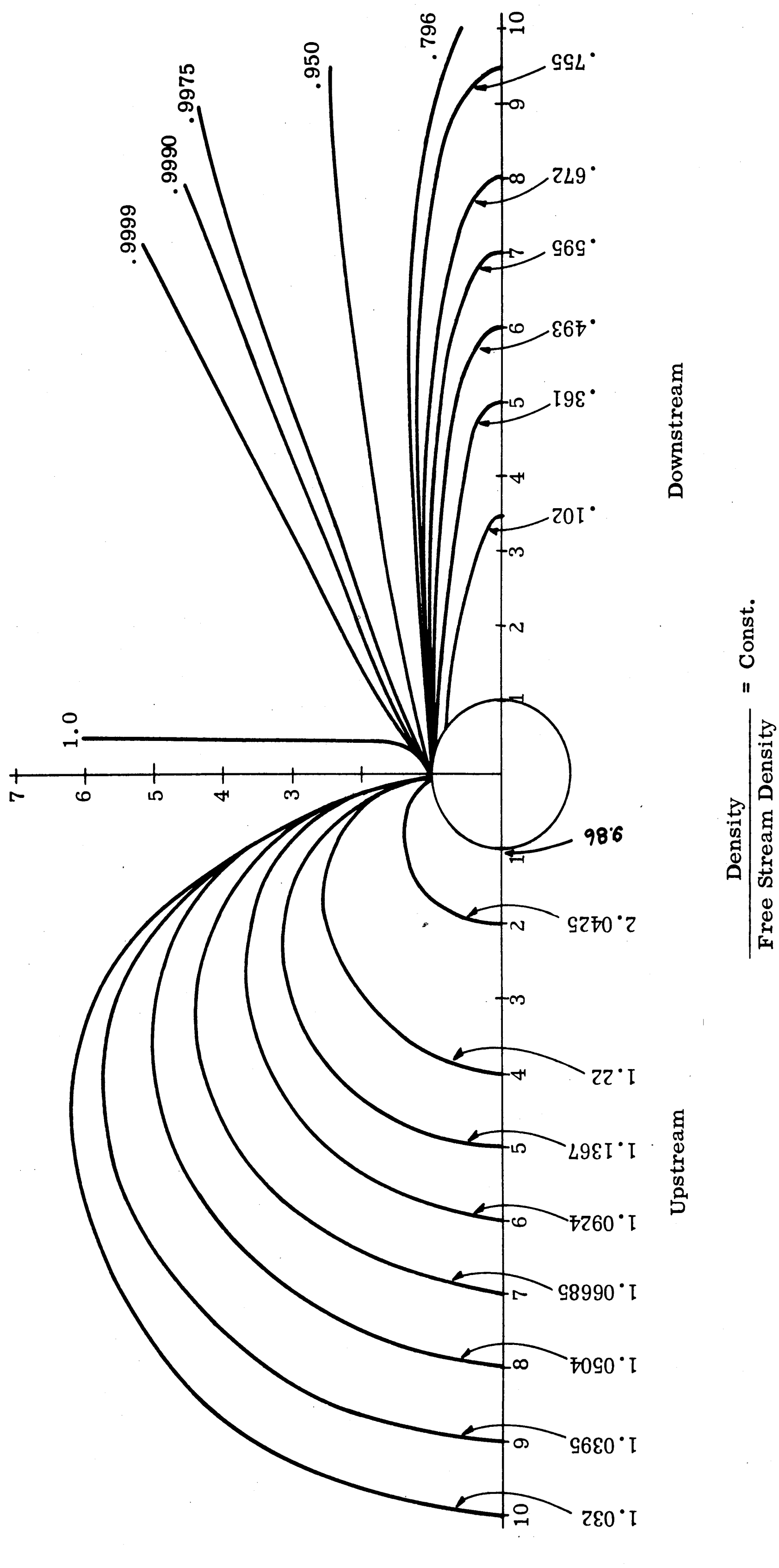

Figure 4. EQUI-DENSITY CONTOURS

meter. Only the λ = 15m and λ = 6.3 meter returns are large enough to be of interest. For these wavelengths, the major part of the region in which the density gradients are large all contribute in phase except for the 180° phasing effect due to the change in sign of N-n ahead and behind the sphere. For these wavelengths the factors which express the asymmetry of the problem about $\Theta = 90^{\circ}$ do not play an important role so that the data for $\Theta = 52^{\circ}$ can be used for $\Theta = 128^{\circ}$ and the σ's for $\Theta = 75^{\circ}$ are essentially those for $\Theta = 105^{\circ}$.

Table III
σ in cm^2

Region	Θ	λ = 15m	λ = 6.3m	λ = 1m
z > 0 (behind)	52°	1.6	.09	----
	75°	9.3	.5	18×10^{-6}
	90°	12.	1.3	53×10^{-6}
z < 0 (ahead)	52°	18.	.95	----
	75°	13.	.58	31×10^{-6}
	90°	12.	.49	180×10^{-6}
$-\infty < z < \infty$ (entire cloud)	52°	32.	1.5	----
	75°	19.	1.7	97×10^{-6}
	90°	.04	.21	74×10^{-6}
$-\infty < z < \infty$ (entire cloud with power contributions from z > 0 and z < 0 added (i.e., average result for random relative phase)	52°	20.	1.0	----
	75°	23.	1.1	49×10^{-6}
	90°	24.	1.8	230×10^{-6}

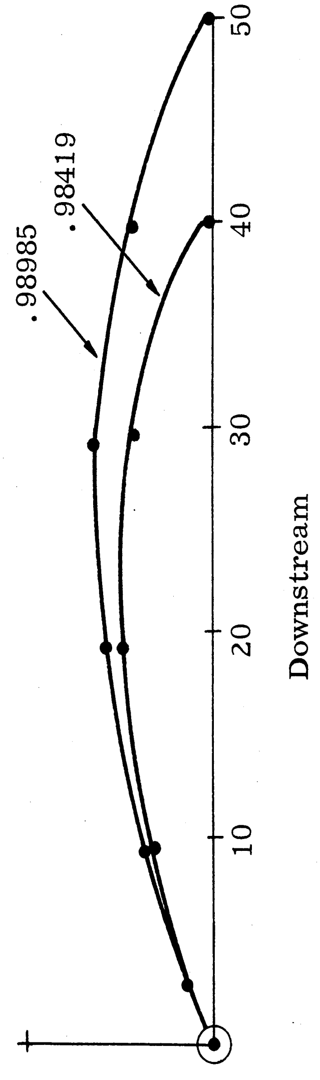

$\frac{\text{Density}}{\text{Free Stream Density}} = \text{Const.}$

Figure 5.

It is of interest to compare these results with a comparable cross section estimate obtained by Davis [13] in a much cruder but far simpler fashion. Davis neglected the density build-up ahead of the sphere and assumed the electrons were completely swept out of a cylindrical column one sphere diameter wide. For this assumption his computations led to a length estimate of 10 sphere diameters behind the sphere. The radar return from such a cavity is that of a column of electrons embedded in a vacuum and of electron number density given by the unperturbed number density. This number of electrons per unit volume was then referred to an equivalent line density and the problem replaced by that of coherent scattering by a line source. It is not clear in [13] but Davis apparently used a wavelength of 15m. To scale Davis' numerical result of $\sigma = .1\ cm^2$ for a .25 m radius sphere in a medium of $n = 10^{12}/m^2$ to the present 1 m radius sphere problem his equivalent line density ($2 \times 10^9/cm$) is scaled by $(100/25)^2 = 16$ and the fact that σ is proportional to line density squared leads to a scale factor of 256 or $\sigma = 25.6\ cm^2$.

An instructive insight into the behavior of the perturbation at various distances ahead or behind the sphere is furnished by a plot of the contribution to the volume integral of the various axial stations; i.e., a plot of

$$S(z) = \int_0^\infty \rho\, d\rho \left(\frac{N}{n} - 1 \right) J_0 \left[2k\rho \sin\theta \right]$$

vs z. A typical graph (for the $\lambda = 6.3$m, $\Theta = 90^o$ case) is furnished in Figure 6. The somewhat odd transition in S(z) as z crosses the origin reflects the fact that N within the sphere is zero. To complete the volume integration this function is to be multiplied by $\exp\left[2ik\left(\frac{z^2}{2R} - z\cos\theta\right)\right]$ and integrated. It is clear that as k increases the rate of oscillation of the exponential will increase and the net contributions from both regions $z > 0$ and $z < 0$, will rapidly decrease.

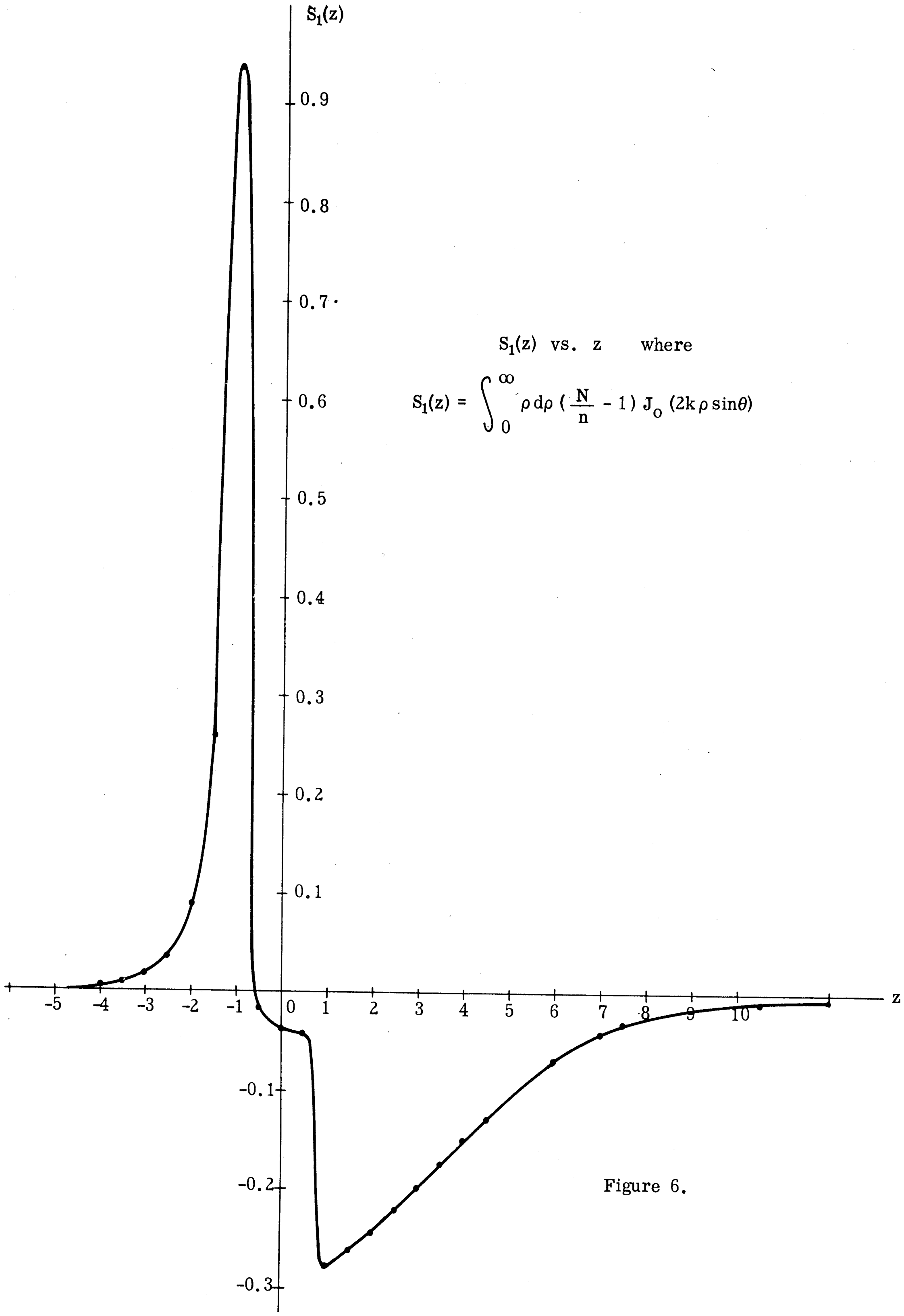
$S_1(z)$
0.9
0.8
0.7
0.6
0.5
0.4
0.3
0.2
0.1
-0.1
-0.2
-0.3
-5 -4 -3 -2 -1 0 1 2 3 4 5 6 7 8 9 10
z
$S_1(z)$ vs. z where
$S_1(z) = \int_0^\infty \rho \, d\rho \left(\frac{N}{n} - 1\right) J_o \left(2k\rho \sin\theta\right)$

Figure 6.

Acknowledgements

The authors would like to thank Professor K.M. Siegel for suggesting the physical bases which enabled the postulate of a neutral gas to be used for determining the ion and electron distributions. The authors would also like to acknowledge helpful discussions with Professor G.E. Uhlenbeck and Professor P.C. Clemmow. Finally, the authors wish to acknowledge the help of Larry B. Evans in coding the formulas for computation and to express their appreciation to The University of Michigan Computing Center, directed by Professor R.C.F. Bartels, for the computing time necessary to complete this work.

Appendix

The Reduction of the "Oseen-Like" Linearized Equations of Motion for an Ionized Medium

by

C. L. Dolph

The problem of the flow in which a sphere is immersed has always been a difficult one in fluid mechanics. Thus, for the case of a sphere with cavitation in an ideal fluid, [14] the flow has been solved only approximately by use of sources leading to a potential $\phi = U(r \cos\theta + a^2/r^2)$ and a stream function $\psi = U\left[\frac{1}{2} r^2 \sin^2\theta - 2a^2 \sin^2(\theta/2)\right]$, in a spherical coordinate system a, θ, ϕ with origin at the sphere center. In addition, the fluid is removed bodily from the cavity. Similarly for viscous flows, there are only the classical solutions of Stokes and Oseen. It is the philosophy of the latter which is of interest here for it is a linearization about the free stream velocity.

For an ionized medium the problem of the sphere has been solved only for point sources (Kraus and Watson [2] and P. Greifinger [3]) on the basis of linearized theory starting from the transport equation, and for spherical probes (Bernstein and Rabinowitz [9]) by use of orbital analysis and assumed mono-energetic distributions.

The starting point for our remarks is the interesting report by R. Pappert [4] who examines the Kraus and Watson solution and deduces it from the Bohm-Pines Theory of the so-called random phase approximation in which the interaction terms in the Fourier expansion of the Coloumb forces are neglected. (Bohm and Pines [5]). In addition to this he deduces the equations of Bohm and Pines from the linearized equations of motion and continuity for ions and electrons and poisson's equation. As in Oseen's treatment, these equations are linearized about the particle in a reference frame moving with it at a constant velocity. In addition, an isothermal equation of state is assumed.

In view of the similarity of these equations to those used by Oseen in his treatment of the flow past a sphere as well as the difficulties associated with such flows in general, it seems worthwhile to attempt a generalization of Oseen's method for this problem. In this Appendix we successfully complete the first step in this program - namely, the reduction of the system of nine scalar equations for the ion and electron velocities, and their respective densities and the static potential by the introduction of two scalar potentials. (Unlike Oseen's case, two scalar potentials must be used since the ions and electrons satisfy separate equations of motion and of continuity because internal static fields are allowed.)

Our starting point is the system of Pappert generalized to include an interaction term proportional to the relative velocity, a scalar viscosity and a gravitational potential, which may be written as follows if the x_1-direction is taken as the direction of rectilinear motion of the sphere.

$$v_o \frac{\partial v_k^+}{\partial x_1} + \frac{kT^+}{m^+\rho_o} \frac{\partial \rho^+}{\partial x_k} + \frac{e}{m^+} \frac{\partial \phi}{\partial x_k} = + \frac{e}{c}(v_e - v_i) + \frac{\mu}{m\rho_o} \sum \frac{\partial^2 v_k}{\partial x_\alpha \partial x_\alpha} - \frac{\partial G}{\partial x_k} \tag{1}$$

$$v_o \frac{\partial v_k^-}{\partial x_1} + \frac{kT^-}{m^-\rho_o} \frac{\partial \rho^-}{\partial x_k} - \frac{e}{m^-} \frac{\partial \phi}{\partial x_k} = - \frac{e}{c}(v_e - v_i) + \frac{\mu}{\rho_o m} \sum \frac{\partial^2 v_k}{\partial x_\alpha \partial x_\alpha} - \frac{\partial G}{\partial x_k} \tag{2}$$

$$\sum_{j=1}^{3} \frac{\partial v_k^+}{\partial x_k} + \frac{1}{\rho_o} v_o \frac{\partial \rho^+}{\partial x_1} = 0 \tag{3}$$

$$\sum_{j=1}^{3} \frac{\partial v_k^-}{\partial x_k} + \frac{1}{\rho_o} v_o \frac{\partial \rho^-}{\partial x_1} = 0 \tag{4}$$

$$\nabla^2 \phi = - 4\pi e \left(\rho^+ - \rho^-\right) \tag{5}$$

In these equations

the electron flow velocity $= -v_o \bar{i} + v^-$

the ion flow velocity $= -v_o \bar{i} + v^+$

the ambient electron density = the ambient ion density $= \rho_o$

the electron density $= \rho_o + \rho^-$

the ion density $= \rho_o + \rho^+$

the electron mass $= m^-$

the ion mass $= m^+$

the electrostatic potential $= \phi$

the unit vector in the x_1 direction $= \bar{i}$.

This system of equations is readily deduced from those given by Spitzer (Physics of Fully Ionized Gases) when an isothermal equation of state is assumed. (Note that equations (1) and (2) must be added to each other to give the full equation of motion.)

To reduce this system let us make the assumption that

$$v_k^{\pm} = \frac{\partial^2 \psi^{+}}{\partial x_1 \partial x_k} . \qquad (6)$$

This implies that the flow is irrotational. Inserting this into equation (3) with the plus superscript, and into equation (4) with the minus superscript, we find

$$\sum_{k=1}^{3} \frac{\partial^3 \psi^{\pm}}{x_1 (x_k)^2} + \frac{v_o}{\rho_o} \frac{\partial \rho^{\pm}}{\partial x_1} = \frac{\partial}{\partial x_1} \left[\nabla^2 \psi^{\pm} + \frac{v_o}{\rho_o} \rho^{\pm} \right] = 0.$$

Thus these equations will be satisfied if we set

$$\rho^{\pm} = - \frac{\rho_o}{v_o} \nabla^2 \psi^{\pm} . \qquad (7)$$

Inserting these values into equation (5) we find that

$$\nabla^2 \phi = 4\pi \frac{e\rho_o}{v_o} \left[\nabla^2 \psi^+ - \nabla^2 \psi^- \right].$$

Thus this equation will be satisfied if we set

$$\phi = 4\pi \frac{e\rho_o}{v_o} \left[\psi^+ - \psi^- \right] + \text{arbitrary harmonic function.} \qquad (8)$$

We ignore this arbitrariness in the sequel, although its inclusion would cause no difficulties.

Inserting (6), (7) and (8) into equations (1) and (2) yields:

$$v_o \frac{\partial^3 \psi^\pm}{\partial x_1^2 \partial x_k} - \frac{kT^\pm}{m^\pm v_o} \frac{\partial}{\partial x_k} \nabla^2 \psi^\pm \pm \frac{4\pi e^2}{m^\pm} \frac{\beta_o}{v_o} \frac{\partial}{\partial x_k} \left[\psi^+ - \psi^- \right]$$

$$= \frac{e}{c} \left(\frac{\partial^2 \psi^+}{\partial x_1 \partial x_k} - \frac{\partial^2 \psi^-}{\partial x_1 \partial x_k} \right) + \frac{\mu}{m^+ \rho_o} \frac{\partial^4 \psi^+}{\partial x_\alpha \partial x_\alpha \partial x_i \partial x_k} - \frac{\partial^2 G}{\partial x_k}$$

$$= \frac{\partial}{\partial x_k} \left\{ v_o \frac{\partial^2 \psi^\pm}{\partial x_1^2} - \frac{kT^\pm}{m^\pm v_o} \nabla^2 \psi^\pm \pm \frac{4\pi e^2}{m^\pm} \frac{\rho_o}{v_o} \left[\psi^+ - \psi^- \right] \right\}$$

$$= \frac{\partial}{\partial x_k} \left\{ \frac{e}{c} \left[\frac{\partial^2 \psi^+}{\partial x_1} - \frac{\partial^2 \psi^-}{\partial x_1} \right] + \frac{\mu}{m^+ \rho_o} \frac{\partial^3 \psi^\pm}{\partial x_1 \partial x_\alpha \partial x_\alpha} - G \right\}$$

Thus these equations will be satisfied if $\psi^{\pm}$ satisfies

$$v_o^2 \frac{\partial^2 \psi^\pm}{\partial x_1^2} - \frac{kT^\pm}{m^\pm} \nabla^2 \psi^\pm \pm \frac{4\pi e^2 \rho_o}{m^\pm} \left[\psi^+ - \psi^- \right] = 0$$

$$= \left\{ \pm \frac{e}{c} \left[\frac{\partial^2 \psi^+}{\partial x_1} - \frac{\partial^2 \psi^-}{\partial x_1} \right] + \frac{\mu}{m^+ \rho_o} \frac{\partial^2 \psi^\pm}{\partial x_1 \partial x_\alpha \partial x_\alpha} - G \right\}.$$

If the interaction, scalar viscosity and gravitational potential are neglected, these equations reduce to

$$\left[\frac{kT^+}{m^+} \nabla^2 - v_o^2 \frac{\partial^2}{\partial x_1^2} - \frac{4\pi e^2 \rho_o}{m^+} \right] \psi^+ = \frac{4\pi e^2 \rho_o}{m^+} \psi^-$$

$$\left[\frac{kT^-}{m^-} \nabla^2 - v_o^2 \frac{\partial^2}{\partial x_1^2} - \frac{4\pi e^2 \rho_o}{m^-} \right] \psi^- = \frac{4\pi e^2 \rho_o}{m^-} \psi^+$$

we see that the general system as well as the reduced system may be uncoupled easily. For example, for the reduced system, we have

$$\left[\frac{kT^-}{m^-} \nabla^2 - v_o^2 \frac{\partial^2}{\partial x_1^2} - \frac{4\pi e^2 \rho_o}{m^-} \right] \left[\frac{kT^+}{m^+} \nabla^2 - v_o^2 \frac{\partial^2}{\partial x_1^2} - \frac{4\pi e^2 \rho_o}{m^+} \right] \psi^+ =$$

$$= \frac{4\pi e^2 \rho_o}{m^+} \left[\frac{kT^-}{m^-} \nabla^2 - v_o^2 \frac{\partial^2}{\partial x_1^2} - \frac{4\pi e^2 \rho_o}{m^-} \right] \psi^- = \frac{16\pi^2 e^4 \rho_o^2}{m^+ m^-} \psi^+$$

This may be simplified to become

$$\left\{\left(\frac{kT^-}{m^-}\nabla^2 - v_o^2\frac{\partial^2}{\partial x_1^2}\right)\left(\frac{kT^+}{m^+}\nabla^2 - v_o^2\frac{\partial^2}{\partial x_1^2}\right) + \frac{4\pi e^2\rho_o k}{m^+ m^-}(T^- + T^+)\nabla^2 - \right.$$

$$\left. - 4\pi e^2\rho_o\left(\frac{1}{m^-} + \frac{1}{m^+}\right) v_o^2\frac{\partial^2}{\partial x_1^2}\right\}\psi^+ = 0.$$

A similar process may be applied to ψ^-. We hope to be able to accomplish the next step in the Oseen formulation which consists in finding simple singular solutions of these equations. This matter is now under investigation.[+]

The reduced equations are identical with those treated by Pappert. Even if viscosity, and interaction are allowed the full system admits a partial separation in any coordinate system in which there is no coupling with the x_1-direction if it is assumed that the functional form of the dependence on the other coordinates is the same for both the ions and the electrons. This assumption still permits different behavior for the ions and electrons since the separation constants can be different for them.

[+] It now appears that this process can be carried through (see a forthcoming paper by C. L. Dolph, R. F. Goodrich).

References

1. H. Brysk, Journ. Geophys. Res., 63, pp. 693-716, 1958.

2. L. Kraus and K.M. Watson, Physics of Fluids, 1, pg. 480, 1958.

3. P. Greifinger, Rand Report R339, Paper No. 19, June 1959.

4. R. Pappert, Convair Report ZPH-026, December 1958.

5. D. Pines and R. Bohm, Phys. Rev., 85, pg. 338, 1952.

6. C.S. Wang Chang, University of Michigan, Engineering Research Institute Report CM-654, December 1950.

7. L. Spitzer, Jr., "Physics of Fully Ionized Gases", Interscience, New York, 1956.

8. C.L. Dolph and R.K. Osborn, University of Michigan Radiation Laboratory Memo No. 2764-547-M, 1959.

9. I.B. Bernstein and I.N. Rabinowitz, Physics of Fluids, 2, pg. 112, 1959.

10. Staedler and Zurich, NACA TN 2423, July 1951.

11. F.C. Hurlbut, Rand Report R339, Paper 21, June 1959.

12. A. Erdelyi, et al., Higher Transcendental Functions, Vol. II, McGraw-Hill, New York, 1953. Eq. 27, pg. 92.

13. A. Davis, Proceedings of the Conference on Interaction of Satellites with the Ionosphere, Naval Research Laboratory, pp. 33, 34, March 28, 1958.

14. W. Bauer, Ann. der Phys. 82, pg. 1014, 1927.

15. M. L. Barasch, H. Brysk, J. W. Crispin, Jr., B. A. Harrison, T. B. A. Senior, K. M. Siegel, H. Weil and V. H. Weston, "Studies in Radar Cross Sections XXIV - Radar Cross Section of a Ballistic Missile - IV: The Problem of Defense", (2778-1-F, April 1959), AF30(602)-1853. SECRET.